

# Analytical Methods

Accepted Manuscript



This is an *Accepted Manuscript*, which has been through the RSC Publishing peer review process and has been accepted for publication.

*Accepted Manuscripts* are published online shortly after acceptance, which is prior to technical editing, formatting and proof reading. This free service from RSC Publishing allows authors to make their results available to the community, in citable form, before publication of the edited article. This *Accepted Manuscript* will be replaced by the edited and formatted *Advance Article* as soon as this is available.

To cite this manuscript please use its permanent Digital Object Identifier (DOI®), which is identical for all formats of publication.

More information about *Accepted Manuscripts* can be found in the [Information for Authors](#).

Please note that technical editing may introduce minor changes to the text and/or graphics contained in the manuscript submitted by the author(s) which may alter content, and that the standard [Terms & Conditions](#) and the [ethical guidelines](#) that apply to the journal are still applicable. In no event shall the RSC be held responsible for any errors or omissions in these *Accepted Manuscript* manuscripts or any consequences arising from the use of any information contained in them.

## Chitosan-based Polyaniline-Au Nanocomposite Biosensor for Determination of Cholesterol

*Monika Srivastava<sup>1</sup>, S. K. Srivastava<sup>2</sup>, N. R. Nirala<sup>3</sup> and Rajiv Prakash<sup>1\*</sup>*

<sup>1</sup>School of Materials Science and Technology, Indian Institute of Technology, Banaras Hindu University, Varanasi-221005, India

<sup>2</sup>Department of Physics, MMV, Banaras Hindu University, Varanasi-221005, India

<sup>3</sup>Department of Zoology, Banaras Hindu University, Varanasi-221005, India

### Abstract

Polyaniline-gold (PAni-Au) nanocomposite is chemically synthesized and impregnated in chitosan matrix for immobilization of cholesterol oxidase on an indium tin oxide-coated glass plate for development of cholesterol biosensor. PAni-Au nanocomposite is characterized for structural and thermal properties. Further PAni-Au nanocomposite is used for cholesterol oxidase immobilization and linkage is examined by FTIR. The nanocomposite is used to form a modified bioelectrode by immobilizing cholesterol oxidase in chitosan matrix and examined under optical microscope for uniformity and morphological studies. Modified bioelectrode (ChOx/PAni-Au-CH/ITO) is used to detect cholesterol by using voltammetric technique with redox mediator. The sensor exhibits linearity in a wide range of 50–500 mg/dL with detection limit as 37.89 mg/dL, sensitivity as  $0.86 \mu\text{A mg/dL}^{-1}$  and a shelf life of more

than 3 weeks when stored at 4 °C. Voltametric studies have also been carried out with common possible interferents. Responses are recorded to get enzyme–substrate kinetics for the biosensor and found as  $K_m = 10.84$  mg/dL. The low value of  $K_m$  indicates that the prepared nanocomposite is facilitating the enzymatic reaction and enzymatic activity. Excellent immobilization and enzyme–substrate reactions show distinct advantage of this matrix over other matrixes used for cholesterol biosensors. The novelty of the prepared electrode lies in its reusability, higher sensitivity, better shelf life, and accuracy.

**Keywords:** Cholesterol sensor, Polyaniline, Polyaniline-Au nanocomposite, Chitosan

\* *Author for Correspondence* E-mail: rprakash.mst@iitbhu.ac.in, Tel: + 91-542-2307047, + 91-9935033011, Fax: + 91-542-2368707

## 1 Introduction

Biosensors have attracted great interest because of their potential applications in clinical diagnostics, environmental, and bioprocess monitoring, etc. [1–5]. The operation of a biosensor involves various factors like electrode material and morphology, compatibility with biosensing molecules, immobilization method, biomolecule–analyte interaction after immobilization, etc. However, effective immobilization and electrical contact of redox biomolecules/enzymes with the surface of the electrode is still a challenge. Conducting polymers have been observed as suitable matrixes for immobilization of various chemicals and biomolecules [1, 3, 6, 7]. Among various conducting polymers, polyaniline [1] has attracted much attention in scientific community because of its excellent properties and stability [8, 9]. However, instead of polymer alone, the polymer–metal nanocomposites have been found as a promising area due

to synergic effect of the two components – one large surface area due to small-sized particles and other the flexible polymer matrix for stable immobilization [10–12]. In literature, several papers have been reported about application of nanocomposites in biosensors [13–16]. Different types of biomolecules like enzymes, protein, and DNA have been immobilized on the polyaniline-modified electrode and their performances for various analytes have been reported [17–20]. PANi-metal nanoparticle composites show enhanced sensing and catalytic capabilities as compared to pure PANi [21–24].

Among various biomolecule estimations, cholesterol estimation has got much more attention [25–34] because of the possibility of coronary heart diseases like hypertension, atherosclerosis, and myocardial infarction due to increased level of blood cholesterol. Very recently, Saini *et al.* [28] have reported a novel nanocomposite coupled with cholesterol oxidase (ChOx) and horseradish peroxidase (HRP) and have explored this bienzymatic nanocomposite for amperometric cholesterol biosensor. Pesqueira *et al.* have recently presented a novel biosensing platform for cholesterol using cholesterol oxidase and polyaniline [29]. Malhotra *et al.* have also reported the covalently immobilized cholesterol oxidase onto electrophoretically deposited conducting polymer film from nanostructured polyaniline colloidal suspension and in another paper, nanocomposite films of PANi and multiwalled carbon nanotubes (MWCNTs) are used for covalent immobilization of ChOx for cholesterol sensing [30, 31]. Khan *et al.* immobilized ChOx on PANi with Triton X-100 and Wang *et al.* also immobilized ChOx on PANi and used the prepared electrodes for determining cholesterol [33]. Abdelwahab *et al.* have achieved direct electrochemistry of ChOx and have further used it for a cholesterol biosensor [34]. However,

in all these cases researchers always felt the importance of immobilization of biomolecules/enzymes and compatibility of electrode materials with biomolecules.

In literature, it is seen that among different biopolymers, chitosan (CH) along with nanoparticles has been found to be a stabilizing agent for enzyme immobilization because of its excellent film-forming ability, mechanical strength, biocompatibility, cost effectiveness, etc. Moreover, amino groups of CH provide a hydrophilic side which is compatible with the biomolecules [35–37]. In view of sensors developed earlier and recent developments in this area, we have used chitosan with PAni-Au nanocomposite as the immobilization matrix for cholesterol oxidase (ChOx) in order to develop a sensitive and stable cholesterol biosensor.

## 2 Materials and Methods

### 2.1 Chemical Reagents

Cholesterol oxidase (ChOx; EC 1.1.36, from *Pseudomonas fluorescens*) with specific activity of 24 U/mg, triton X-100, chitosan, potassium ferricyanide, potassium ferrocyanide, and cholesterol were obtained from Sigma Aldrich (USA). Gold chloride was obtained from SRL (Sisco), India. All other chemicals used were of analytical grade.

### 2.2 Instrumental Details

Fourier transform infrared spectroscopy (FTIR) was performed on ThermoScientific FTIR (Thermo Nicolet 6700, Germany).

X-ray diffraction (XRD) was performed on 18 kW rotating anode ( $\text{Cu}_{k\alpha}$ ) Rigaku X-ray diffractometer (wavelength 0.154 nm, Japan).

Scanning electron microscopy (SEM) and energy-dispersive X-ray spectroscopy (EDX) were carried out using Zeiss (AG-Supra 40, Germany) at operating voltage of 5.0 kV. Thermal analysis was carried out using a thermal gravimetric analyzer (TGA) (Mettler-Toledo, Switzerland) at a heating rate of 20 °C/min under nitrogen atmosphere. Transmission electron microscopy (TEM) was performed on Tecnai 20 G<sup>2</sup> operated at 200 kV for structural analysis. Cyclic voltammetry (CV) was performed using a conventional three-electrode cell set up with a platinum foil as counter electrode, Ag|AgCl (saturated KCl) as reference electrode and Indium tin oxide (ITO), modified with composite as working electrode (geometrical area 1 cm<sup>2</sup>) with Autolab (PGSTAT101, Metrohm, The Netherlands). The electrolyte used was phosphate buffer solution of 0.05 M and 7.4 pH value. Electrochemical impedance spectroscopy (EIS) measurements were conducted on electrochemical workstation (CHI-7041C, USA).

## 2.3 Experimental Details

### 2.3.1 Synthesis of PANi-Au Nanocomposites

In the synthesis scheme of PANi-Au nanocomposite, two solutions (A and B) were prepared as discussed below.

Solution A was prepared by dissolving 200 μL of aniline monomer in 10 mL of 0.5 M HCl while solution B was prepared by dissolving 135 mg of HAuCl<sub>4</sub> in 10 mL of 0.5 M HCl. This concentration was calculated to keep the aniline monomer to HAuCl<sub>4</sub> molar ratio of 5:1. Solution B was added dropwise to solution A, under stirring condition at temperature below 10 °C. Dark green precipitates appeared after sometime. After complete polymerization (24 h), precipitates were collected by centrifugation and then

washed several times with distilled water to remove monomer and oxidant. The dried sample was used for characterization and sensor application. It was also found that the prepared composite had retained its property even after a year.

### ***2.3.2 Preparation of a PAni-Au-CH/ITO Electrode***

The PAni-Au nanocomposite already prepared was used with chitosan as a matrix for the preparation of PAni-Au-CH/ITO electrode. A chitosan solution was prepared by dissolving CH (50 mg) in 10 mL of distilled water and 2 mL of acetic acid solution. The measured amount of PAni-Au nanocomposite was dispersed in the CH solution. Then, on the already hydrolyzed Indium tin oxide (ITO)-coated glass plate of  $1 \times 2 \text{ cm}^2$  area, 10  $\mu\text{L}$  of the aforesaid solution was spin coated to get coating over an area of  $1 \times 1 \text{ cm}^2$  only (rest of the area was masked to get electrical contact). The coated ITO was kept for drying in an oven before making electrical contacts using silver paint (room dry paint).

### ***2.3.3 Preparation of a ChOx/PAni-Au-CH/ITO Electrode***

In the next step, bioelectrode for sensing cholesterol with enzyme cholesterol oxidase was prepared. A 10  $\mu\text{L}$  of freshly prepared solution of cholesterol oxidase ( $1 \text{ mg mL}^{-1}$ ) in phosphate buffer (0.2 M, pH 7.0) was mechanically spread over the PAni-Au-CH/ITO electrode to get immobilization in CH matrix. Cartoon representation of this electrode is shown in Figure 1, where green-color structure represents PAni, red spot indicates Au nanoparticle, and blue curve line shows chitosan. The ChOx/PAni-Au-CH/ITO

bioelectrode was kept undisturbed at room temperature for about 12 h in a humid chamber. Finally, the bioelectrode was washed with phosphate buffer (0.2 M, pH 7.0) to remove any unbound enzyme from the electrode surface.

## Figure 1

### 2.4 Electrochemical Measurement

Electrolytic solution for electrochemical measurement was freshly prepared by dissolving potassium ferricyanide  $K_3[Fe(CN)_6]$  (5 mM) and potassium ferrocyanide  $K_4[Fe(CN)_6]$  (5 mM) in 100 mL of phosphate buffer saline (PBS) (0.2 M, pH 7.0). Then, prepared electrodes were characterized by CV and finally used for, sensing of different concentrations of cholesterol.

### 2.5 Preparation of Cholesterol Solution

Measured quantity of cholesterol was taken in 1 mL triton and mild heating was done for dissolving cholesterol. After complete dissolution of cholesterol, 9 mL of distilled water was added to get a transparent solution.

## 3 Results and discussion

### 3.1 Characterization of PANi-Au Nanocomposite

XRD of PANi and PANi-Au nanocomposite is shown in Figure 2. PANi (curve a) exhibited broad peaks at  $2\theta = 25^\circ$ , indicating its amorphous nature. Polyaniline-Au nanocomposite (curve b) shows the background of pure polymer in addition with a few small peaks

indicating the presence of Au nanoparticles. It exhibited four peaks at  $2\theta = 38.7, 45.0, 65.3$  and  $78.2$  corresponding to the (111), (200), (220), and (310) Bragg reflections of reduced Au crystallites respectively [38, 39]. This result was also concurrent with JCPDS (card no.040784).The remaining peaks are not visible due to low intensity factor with respect to (111)plane which is suppressed in the polymer background. In addition to these peaks, two small sharp peaks also appeared below  $30^\circ$  probably due to alignment of polyaniline chains in the vicinity of Au nanoparticles as also reported earlier [40].

### Figure 2

Further morphology and elemental analysis of the nanocomposite was carried out under SEM equipped with energy dispersive X-ray spectroscopy (EDS). Globular morphology of PANi was observed in the PANi-Au nanocomposite as shown in Figure 3. However, gold nanoparticles could not be visualized but were confirmed in the elemental analysis (inset: Figure 3).

### Figure 3

Thermal gravimetric analysis (TGA) of pure PANi and PANi-Au nanocomposite is illustrated in Figure 4. Curve a represents pure PANi and curve b represents PANi-Au nanocomposite. From the figure, it is evident that thermal stability of prepared nanocomposite is better as compared to pure PANi. From the thermogram, approximate gold content was calculated and found as 7–8%.

### Figure 4

Further, in order to study the presence of Au nanoparticles, TEM characterization was carried out by taking the samples on Au grid. TEM micrograph (Figure 5) clearly demonstrates the nanoparticles in the polymer matrixes. The nanoparticles show the size distribution in the range of 40–60 nm in diameter [24].

## Figure 5

### 3.2 Characterization of Electrode and Bioelectrode

Structural and morphological characterizations were done for the prepared electrode and bioelectrode.

#### 3.2.1 Structural Characterization

Figure 6 shows FTIR spectra of PANi-Au-CH (curve a), ChOx/PANi-Au-CH (curve b), and pure chitosan (curve c). In curve a, the presence of peaks at 1062 and 3412  $\text{cm}^{-1}$  are attributed to B-N<sup>+</sup>=Q stretching and -N-H stretching vibrations of PANi in the nanocomposite. In curve b, peak at 1408  $\text{cm}^{-1}$  is due to C-N axial deformation (amine group band) and at 1644  $\text{cm}^{-1}$  it is due to COO- group in carboxylic acid. Also, a broad band at 3433  $\text{cm}^{-1}$  is because of amide bond present in ChOx. Pure chitosan (curve c) exhibited its characteristic absorption band at 1568  $\text{cm}^{-1}$  because of stretching vibration of the amino group. Another band at 3446  $\text{cm}^{-1}$  is due to N-H symmetric vibration. The peaks at 2857 and 2927  $\text{cm}^{-1}$  are due to C-H vibrations [31, 41]. On comparison of a, b, and c, it is confirmed that the nanocomposite is having ChOx, immobilized in PANi-Au-CH matrix.

## Figure 6

### 3.2.2 Morphological Characterization

The surface morphology of deposited thin film of both PANi-Au-CH/ITO electrode and ChOx/PANi-Au-CH/ITO bioelectrode was investigated under optical microscope (Figure 7). The two images clearly showed the difference between before and after immobilization of enzyme over the surface of nanocomposite electrodes. The bioelectrode (ChOx/PANi-Au-CH/ITO) morphology supported the uniform distribution of ChOx over the surface of PANi-Au-CH.

#### Figure 7

### 3.3 Electrochemical Characterization of Electrode and Bioelectrode

PANi-Au-CH/ITO electrode and ChOx/PANi-Au-CH/ITO bioelectrode have been characterized using CV technique using three-electrode system in a phosphate buffer (PBS) containing a mixture of 5 mM potassium ferricyanide and potassium ferrocyanide. CV responses were obtained for bare ITO, pure PANi, PANi-Au-CH/ITO, and ChOx/PANi-Au-CH/ITO electrodes in the potential range from  $-1$  to  $+1$  V at a scan rate of 100 mV/s as shown in Figure 8. The increase in the cathodic current obtained for pure PANi (0.95 mA, curve b) and PANi-Au-CH/ITO (0.99 mA, curve c) compared to bare ITO electrode (0.63 mA, curve a) indicates that the larger effective area of PANi-Au nanocomposite helps in large-scale redox conversion, resulting increase in redox current which also reflects its enhanced electron transfer property. The decrease in the anodic current obtained for ChOx/PANi-Au-CH/ITO bioelectrode (0.66 mA, curve d) is attributed to the hindrance caused by macromolecular structure of enzymes and their successful immobilization.

**Figure 8****3.3.1 Electrochemical Impedance Studies**

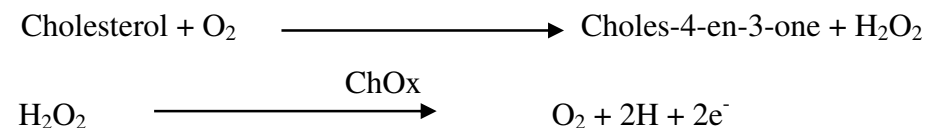
Electrochemical impedance studies (EIS) were conducted to confirm the immobilization of enzyme over the surface of PAni-Au. The results of EIS measurements in Nyquist plot indicated the hindrance provided by the electrode material to the transfer of charge from solution to electrode. Thus, change in the charge-transfer-resistance ( $R_{CT}$ ) value can be correlated to the modification of surface [42]. Figure 9 shows the observed charge-transfer-resistance of bare ITO (curve a), PAni-Au-CH/ITO electrode (curve b) and ChOx/PAni-Au-CH/ITO (curve c). These three curves show clearly that accumulation of charge at the surface of electrode or its charge-transfer property is maximum in bare ITO and it decreases in PAni-Au-CH/ITO electrode and further in ChOx/PAni-Au-CH/ITO bioelectrode as is evident from the inclination of curves towards “Z.” Curve b shows surface electron property near the origin point and at low frequency but with time it shows the diffusion control process as evident by its straight-line part. The observed increase in the value of  $R_{CT}$  is attributed to the hindrance caused by the macromolecular structure of ChOx. The increase in the value of  $R_{CT}$  (curve c) on immobilization of enzyme (ChOx) further confirms the successful uniform immobilization of enzyme on the matrix.

**Figure 9**

### 3.3.2 Study of Electrochemical Response of ChOx/PAni-Au-CH/ITO Bioelectrode

The response of ChOx/PAni-Au-CH/ITO bioelectrode has been studied by CV method as a function of cholesterol concentration.

During the biochemical reaction, cholesterol oxidase catalyzes decomposition of cholesterol into Choles-4-en-3-one and H<sub>2</sub>O<sub>2</sub>.



The response increase in current at positive potential comes from the oxidation of produced H<sub>2</sub>O<sub>2</sub> and the decrease at negative potential originates from the consumption of O<sub>2</sub>. Although the reduction of produced H<sub>2</sub>O<sub>2</sub> will result in the increase of current at negatively applied potentials, it would be entirely counteracted due to the consumption of O<sub>2</sub>.

#### Figure 10

The electrons generated during the biochemical reactions are transferred to the electrode via Fe (III)/Fe (II) redox probe ensuing in signal in the form of current. Figure 10 shows the schematic mechanism of electrochemical sensing of cholesterol on bioelectrode ChOx/PAni-Au-CH/ITO. Cyclic voltammogram response of a ChOx/PAni-Au-CH/ITO bioelectrode with different concentrations of cholesterol (say a–i) is shown in Figure 11. The calibration curve has been fitted between the cholesterol concentration and current value of redox peaks (Figure 12). It is found that magnitude of the current increases linearly as cholesterol concentration increases (sensing range as 25–500 mg/dL) and obeys Eq. (1) below, where  $I_p$  denotes anodic current, A denotes intercept and B denotes slope.

ChOx/PAni-Au-CH/ITO bioelectrode exhibits linearity as 50–500 mg/dL and detection limit as 37.89 mg/dL while sensitivity of ChOx/PAni-Au-CH/ITO bioelectrode has been estimated as  $0.86 \mu\text{A mgdL}^{-1}$  with the regression coefficient of 0.997 and standard deviation as  $1.07867 \times 10^{-5}$ .

$$I_p = 6.07549E^{-4}(A) + 8.55183E^{-7}A \text{ mgdL}^{-1}(B) \times \left\{ \text{cholesterol concentration (mgdL}^{-1}) \right\}. \text{ Eq.(1)}$$

The apparent Michaelis–Menten constant ( $K_m$ ) gives an indication of enzyme–substrate kinetics for the biosensor, which is calculated by Lineweaver–Burk plot, i.e., the graph between inverse of maximum current and inverse of cholesterol concentration and has been found to be 10.84 mg/dL. Lower value of  $K_m$  describes the higher affinity of enzyme with substrate, indicating its biocompatibility and facilitation of the enzymatic reaction.

The results obtained in the present study, along with the results reported in the literature, are summarized in Table 1. The advantage of PAni-Au nanocomposite film over the other matrixes is shown clearly in Table 1, which reveals that the bioelectrode developed in this study can detect cholesterol over a broad range with high sensitivity. It also indicates the enhancement of the bio-electrocatalytic oxidation of cholesterol with lower  $K_m$  value

**Figure 11**

**Figure 12**

**Table 1**

### 3.4 Amperometric Response Studies for Interference, Reproducibility, Reusability, and Shelf Life

Amperometric response studies have been carried out for ChOx/PAni-Au-CH/ITO bioelectrode as a function of interferents, reproducibility, reusability, and storage stability.

#### 3.4.1 Interference Studies

Different possible interferents that are mostly present in blood such as ascorbic acid (0.05 mM), glucose (5 mM), and urea (1 mM) were checked through CV measurements for the prepared electrode (ChOx/PAni-Au-CH/ITO) using cholesterol solution (100 mg/dL) in a 1:1 ratio. Figure 13 shows the effect of interferents on the observed response of the bioelectrode. From Figure 13, the percentage interference (% interference) was calculated and was found a maximum of 21% for ascorbic acid, 15% for glucose, and 17% for urea.

#### Figure 13

#### 3.4.2 Reproducibility and Reusability Studies

The unique feature of the prepared bioelectrode is shown by its consistent results in cyclic voltammogram. ChOx/PAni-Au-CH/ITO were prepared in triplicate sets with each and every parameter being the same, and then the CV was recorded for 400 g/dL concentration of cholesterol in the same condition as described earlier. Figure 14 shows that the results are reproducible. For

reusability experiments are also done with only one electrode and found that it can be used for more than 20 times with nearly 100% efficiency (data not shown) or negligible variation. The reusability of the bioelectrode can be attributed to its robust properties of the transducer matrix. The reusability studies also indicate the advantage of prepared matrix, which offers a favorable microenvironment for enzymes and does not cause denaturing of enzymes.

#### **Figure 14**

#### ***3.4.3 Shelf Life Studies***

The shelf life of ChOx/PAni-Au-CH/ITO bioelectrode has been determined by measuring the response current at 0 and 1 day, then at regular intervals of one week for about a month, if stored at 4 °C when not in use. Figure 15 demonstrates the shelf life of a ChOx/PAni-Au-CH/ITO bioelectrode. The bioelectrode has been found to be stable up to 2 weeks with a variation of 2–3% variation. After 3 weeks, the electrode retains about 90% of cholesterol oxidase activity.

#### **Figure 15**

#### **4 Conclusions**

A novel approach for electrochemical sensing of cholesterol through a ChOx/PAni-Au-CH/ITO bioelectrode is reported and stable sensor is demonstrated and compared with earlier reported sensors. PAni-Au nanocomposite is synthesized and characterized using various tools, viz., XRD, SEM, EDX, TEM, and TGA. This bioelectrode has been successfully utilized for sensing application as cholesterol biosensor. It offers better performance in terms of detection limit, sensitivity, and response time and shows linearity as 50–

500 mg/dL with detection limit as 37.89 mg/dL and sensitivity as  $0.86 \mu\text{A mgdL}^{-1}$ . The value of the apparent Michaelis–Menten constant ( $K_m$ ), which indicates enzyme–substrate interactions, is found to be 10.84 mg/dL. Low value of  $K_m$  for ChOx/PAni-Au-CH/ITO bioelectrode reveals increased enzyme (cholesterol oxidase) –substrate (cholesterol) interactions and indicates distinct advantage of this prepared matrix over other matrixes used for cholesterol biosensor fabrication. The unique features of the ChOx/PAni-Au-CH/ITO nanocomposite bioelectrode are its fabrication and stability, less interference, low  $K_m$  value, fast response time (20 s), excellent reusability, and its usefulness for serum samples. Work is in progress to utilize these electrodes for estimation of cholesterol in serum samples and conduct similar experiments with other enzymes and in the development of other biosensors.

### **Acknowledgments**

One of the authors (MS) is grateful to the Department of Science and Technology (DST), New Delhi, for financial support. MS is also thankful to Dr. P. S. Saxena, Department of Zoology, BHU, Varanasi, for her help extended towards handling of biomaterials and characterization. MS also wants to acknowledge Ashish Kumar, SMST, IIT, BHU, Varanasi, for his kind help whenever needed during the work. The other author (SKS) is thankful to UGC for the financial support.

## References

- 1 Z.M. Tahir, E.C. Alocilja, D.L. Grooms, *Biosensors and Bioelectronics*, 2005, **20**, 1690.
- 2 A. Morrin, O. Ngamna, A.J. Killard, S.E. Moulton, M.R. Smyth, G.G. Wallace, *Electroanalysis*, 2005, **17**, 423.
- 3 S.E. Moulton, P.C. Innis, L.A.P. Kane Maguire, O. Ngamna, G.G. Wallace, *Current Applied Physics*, 2004, **4**, 402.
- 4 S. Mohan, P. Nigam, S. Kundu, R. Prakash, *Analyst*, 2010, **135**, 2887.
- 5 S. Mohan and R. Prakash, *Talanta*, 2010, **81**, 449.
- 6 A. Kumar and R. Prakash, *Catalysis Science & Technology (RSC)*, 2012, **2**, 2533.
- 7 L. Joshi and R. Prakash, *Thin Solid Films*, 2013, **534**, 120.
- 8 H. Ding, M. Wan, Y. Wei, *Advanced Materials*, 2007, **19**, 465.
- 9 B. Gupta and R. Prakash, *Journal of Applied Polymer Science*, 2009, **114**, 874.
- 10 S.H. Yun, S.M. Yoo, B.H. Sohn, J.C. Jung, W.C. Zin, S.Y. Kwak, T.S. Lee, *Langmuir*, 2005, **21**, 3625.
- 11 W. Yan, X. Feng, X. Chen, W. Hou, J.J. Zhu, *Biosensors and Bioelectronics*, 2008, **23**, 925.
- 12 E. Pinter, R. Patakfalvi, T. Fulei, Z. Gingl, I. Dekany, C. Visy, *Journal of Physical Chemistry B*, 2005, **109**, 17474.
- 13 P. P. Joshi, S. A. Merchant, Y. Wang, D. W. Schmidtke, *Analytical Chemistry*, 2005, **77**, 3183.
- 14 S. R. Ali, Y. Ma, R. R. Parajuli, Y. Balogun, W. Y. C. Lai, H. He, *Analytical Chemistry*, 2007, **79**, 2583.
- 15 W. Yan, X. Chen, X. Li, X. Feng, J. J. Zhu, *Journal of Physical Chemistry B*, 2008, **112**, 1275.

- 16 J. Li, X. Lin, *Biosensors and Bioelectronics*, 2007, **22**, 2898.
- 17 J. Kan, X. Pan, C. Chen, *Biosensors and Bioelectronics*, 2004, **19**, 1635.
- 18 G. Bolat , F. Kuralay , G. Eroglu , S. Abaci, *Sensors*, 2013, **13**, 8079.
- 19 N. Zhu, Z. Chang, P. He, Y. Fang, , *Electrochimica Acta*, 2006, **18**, 3758.
- 20 H. Chang, Y. Yuan, N. Shi, Y. Guan, *Analytical Chemistry*, 2007, **79**, 5111.
- 21 A. Kitani, T. Akashi, K. Sugimoto, S. Ito, *Synthetic Metals*, 2001, 121, 1301.
- 22 A. Drelinkiewicz, M. Hasik, M. Kloc, *Catalysis Letters*, 2000, 64, 41-47.
- 23 P. T. Radford, S. E. Creager, *Analytica Chimica Acta*, 2001, **449**, 199.
- 24 W. Yang, J. Liu , R. Zheng, Z. Liu , Y.Dai, G. Chen, S. Ringer, F. Braet, *Nanoscale Research Letters*, 2008, 3, 468.
- 25 S. Aravamudhan, A. Kumar, S. Mohapatra, S. Bhansali, *Biosensors and Bioelectronics*, 2007, **22**, 2289-2294.
- 26 J.C. Vidal, E.G. Ruiz, J.R. Castillo, *Journal of Pharmaceutical and Biomedical Analysis*, 2000, **24**, 51.
- 27 A. Parra, E. Casero, F. Pariente, L. Vazquez, E. Lorenzo, *Sensors and Actuators B*, 2007, **124**, 30.
- 28 D. Saini, R. Chauhan, P. R. Solanki, T. Basu, *ISRN Nanotechnology*, 2012, Volume **2012**, Article ID 102543, 1.
- 29 C. L. Medrano Pesqueira, T. del Castillo-Castro, M. M. Castillo-Ortega, J. C. Encinas, *Journal of Polymer Research*, 2013, **20**, 71.
- 30 C. Dhand, S.P. Singh, S.K. Arya, M. Datta, B.D. Malhotra, *Analytica Chimica Acta*, 2007, **602**, 244.
- 31 C. Dhand ,S. K. Arya, M. Datta , B.D. Malhotra , *Analytical Biochemistry*, 2008, **383**, 194.
- 32 R. Khan, A. Kaushik , A.P. Mishra, *Materials Science and Engineering C*, 2009, **29**, 1399.

- 33 H. Wang, S. Mu, *Sensors and Actuators B*, 1999, **56**, 22.
- 34 A. A. Abdelwahab, M.S. Won, Y.B. Shim, *Electroanalysis*, 2010, **22**, 21.
- 35 Y. Miao and S. N. Tan, *Analyst*, 2000, **125**, 1591.
- 36 M. D. Blankschien, L. A. Pretzer, R. Huschka, N. J. Halas, R. Gonzalez, M. S. Wong, *ACS Nano*, 2013, **7**, 654.
- 37 C. Xu, H. Cai, P. He, Y. Fang, *Analyst*, 2001, **126**, 62.
- 38 D. Yanakieva, M. Tonkova, E. Spiridonov, Z. Vergilov et, P. Penkova, *ArcheoSciences*, 2009, **33**, 45.
- 39 S. K. Pillalamarri, F. D. Blum, A. T. Tokuhira, M. F. Bertino, *Chemistry of Materials*, 2005, **17**, 5941.
- 40 A.K. Singh, L. Joshi, B. Gupta, A. Kumar, R. Prakash, *Synthetic metals*, 2011, **161**, 481.41 F. Tian , Y. Liu, K. Hu, B. Zhao, *Journal of Materials Science*, 2003, **38**, 4709.
- 42 X.L. Luo, J.J. Xu, Q. Zhang, G.J. Yang, H.Y. Chen, *Biosensors and Bioelectronics*, 2005, **21**, 190.
- 43 M. Guo, J. Chen, J. Li, L. Nie, S. Yao, *Electroanalysis*, 2004, **16**, 1992.
- 44 A. Parra, E. Casero, F. Pariente, L. Vazquez, E. Lorenzo, *Sensors and Actuators B*, 2007, **124**, 30.
- 45 H.Y. Wang, S.L. Mu, *Sensors and Actuators B*, 1999, **56**, 22.

**Highlights**

Polyaniline-gold nanocomposite impregnated in chitosan matrix and immobilized with cholesterol oxidase for redox mediator based cholesterol sensor.

**Table 1:** Sensing Characteristics of ChOx/PAni-Au-CH/ITO Bioelectrode along with those Reported in the Literature.

| Immobilization matrix | Sensing element | Method of immobilization | Linearity                                      | Transducer used                     | Sensitivity                                    | Shelf life | $K_m$ value                                    | Ref.         |
|-----------------------|-----------------|--------------------------|--|-------------------------------------|--|------------|--|--------------|
| MWNT                  | ChOx            | Physical entrapment      | 0.5–6 mM or 9–108 mg.dL <sup>-1</sup>          | Amperometric                        | 0.559 $\mu\text{A cm}^{-2}\text{mM}^{-1}$      | -          | -  | [43]         |
| Gold electrode        | ChOx            | Physical adsorption      | 0–2.1 mM or 37.8 mg.dL <sup>-1</sup>           | Amperometric                        | 0.13 $\mu\text{A mM}^{-1}$                     | -          | 2.94 mM or 52.92 mgdL <sup>-1</sup>            | [44]         |
| PAni-MWCNT            | ChOx            | Covalent                 | 1.3–12.9 mM or 23.22–232.74 mgdL <sup>-1</sup> | Amperometric and spectrophotometric | 6800 nA mM <sup>-1</sup>                       | 12 weeks   | -  | [31]         |
| PAni                  | ChOx            | Electrochemical doping   | 0.05–0.5 mM or 0.9–9 mgdL <sup>-1</sup>        | Amperometric                        | -  | 11 days    | 2.27–3.26 mM or 40.86–58.68 mgdL <sup>-1</sup> | [45]         |
| PAni                  | ChOx            | Covalent                 | 25–400 mgdL <sup>-1</sup>                      | Spectrophotometric                  | $7.76 \times 10^{-5}$ Abs. mg <sup>-1</sup> dL | 11 weeks   | 26.14 mgdL <sup>-1</sup> or 1.45 mM            | [30]         |
| NSPAni-AuNP-GR        | ChOx            | Electrochemical          | 35–400 mgdL <sup>-1</sup>                      | DPV                                 | 3.10 $\mu\text{A mg}^{-1}\text{dL}$            | 8 weeks    | 0.02 mM or 0.36 mgdL <sup>-1</sup>             | [28]         |
| PAni-Au-CH            | ChOx            | Covalent                 | 50–500 mgdL <sup>-1</sup>                      | Amperometric                        | 0.86 $\mu\text{A mg}^{-1}\text{dL}$            | 3 weeks    | 10.84 mgdL <sup>-1</sup> or 0.602 mM           | Present work |

**Caption to Figure**

**Fig.1.** Schematic diagram of (a) PANi-Au-CH/ITO electrode (b) ChOx / PANi-Au- CH / ITO bioelectrode

**Fig.2.** XRD of (a) PANi and (b) PANi-Au nanocomposite

**Fig.3.** SEM of PANi-Au nanocomposite, Inset showing EDX of the selected area

**Fig.4 .** TGA curve for (a) pure PANi and (b) PANi-Au nanocomposite

**Fig.5.** TEM micrograph of the PANi-Au nanocomposite . Scale bar is 100 nm

**Fig.6.** FTIR of (a) PANi-Au-CH, (b) ChOx/PANi-Au-CH and (c) chitosan

**Fig.7.** Images of optical microscope of electrode surface (a) PANi-Au-CH/ITO and (b) ChOx/PANi-Au-CH/ITO

**Fig.8.** Cyclic voltammetry of (a) bare ITO electrode (b) ITO modified with pure PANi (c) PANi-Au-CH/ITO electrode and (d) ChOx/PANi- Au-CH/ ITO bioelectrode

**Fig.9.** Impedance spectra of (a) bare ITO ,(b) PANi-Au-CH/ITO and (c) ChOx/PANi-Au-CH/ITO

**Fig.10.** Schematic mechanism of electrochemical sensing of Cholesterol on ChOx /PANi-Au-CH / ITO bioelectrode

**Fig.11.** Cyclic voltammogram response of ChOx /PANi-Au-CH/ITO bioelectrode with different concentrations of cholesterol, say a-i (a to i represents 25,50,100,150,200,250,300,400,500 mg/dL respectively), Inset shows zoom part of the oxidation peak

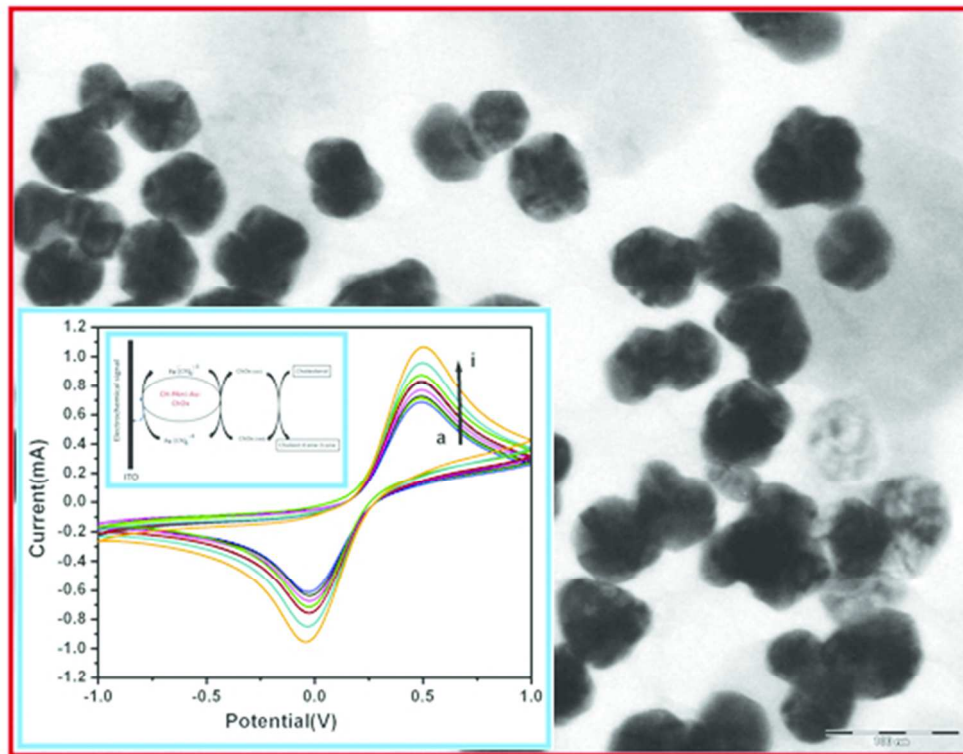
**Fig.12.** Calibration curve for Cholesterol with 3% error bar

**Fig. 13:** Interferent Study of a ChOx/PANi-Au-CH/ITO Bioelectrode.

**Fig. 14:** Reproducibility Curve of ChOx/PANi-Au-CH/ITO Bioelectrode by Cyclic Voltammogram Response Studies with 400 mg/dL Concentrations of Cholesterol (Inset Shows Zoom Part of the Oxidation Peaks to Depict the Clarity of Three Different Curves).

**Fig. 15:** Stability Curve of ChOx/PANi-Au-CH/ITO Bioelectrode by Cyclic Voltammogram Response Studies with 400 mg/dL Concentrations of Cholesterol at 0 (curve b), 1 (curve c), 7 (curve d), 14 (curve e), 21 (curve f) Day while Curve a Is w/o Cholesterol (Inset Shows Zoom Part of the Oxidation Peaks to Depict the Clarity of Individual Curves).

**Table 1.** Sensing characteristics of ChOx/PAni-Au-CH/ITO bioelectrode along with those reported in the literature



Polyaniline-gold nanocomposite impregnated in chitosan matrix and immobilized with cholesterol oxidase for redox mediator based cholesterol sensor.  
47x36mm (300 x 300 DPI)

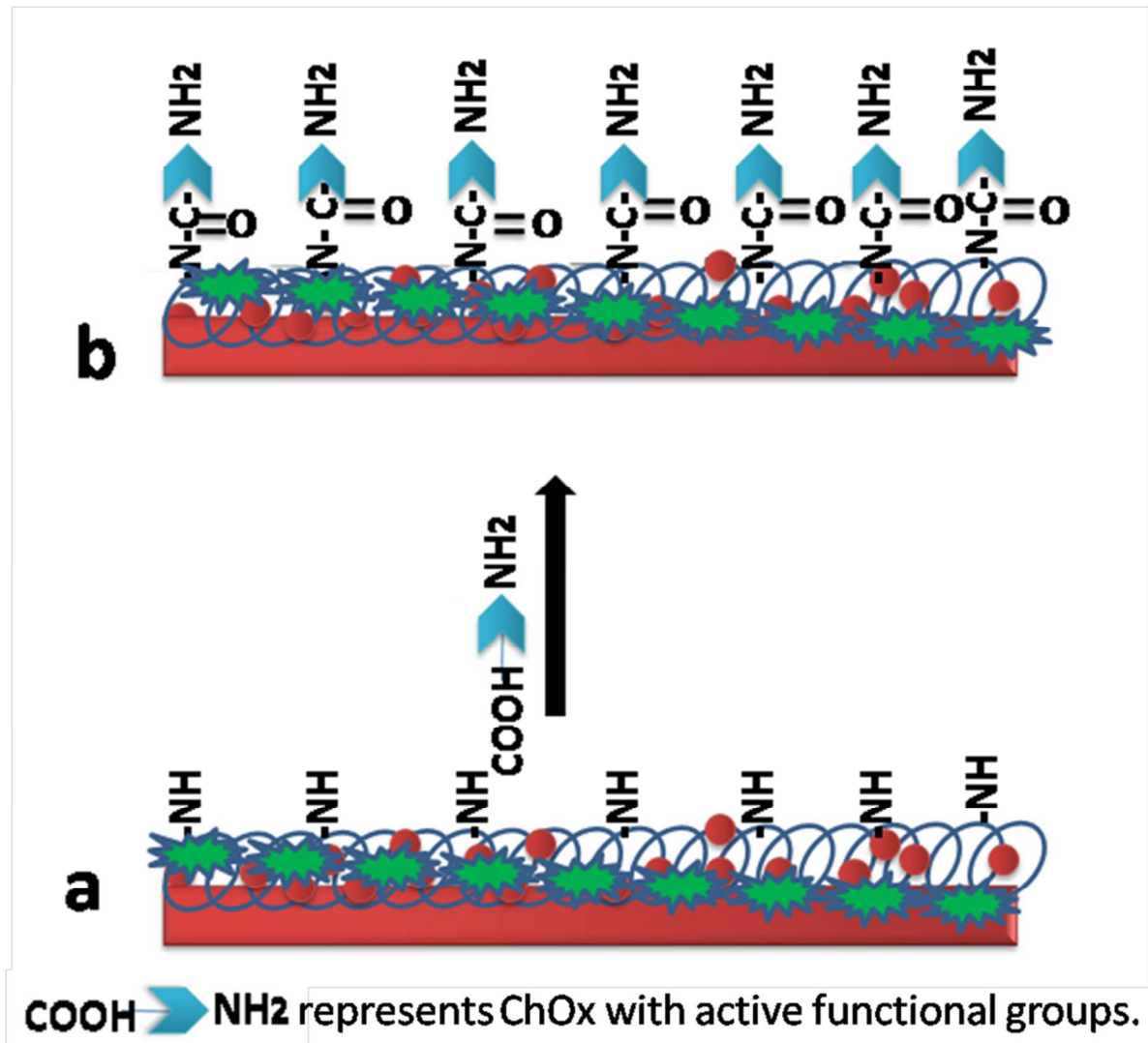


Figure 1

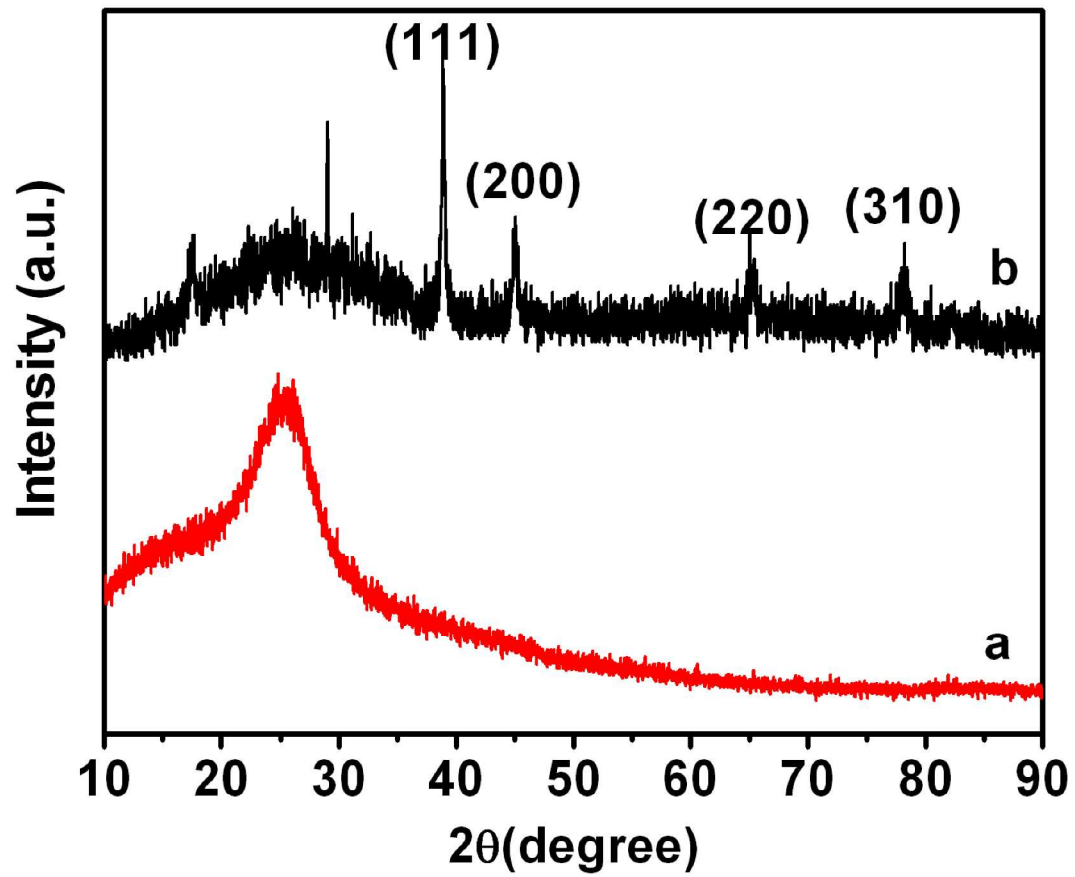


Figure 2

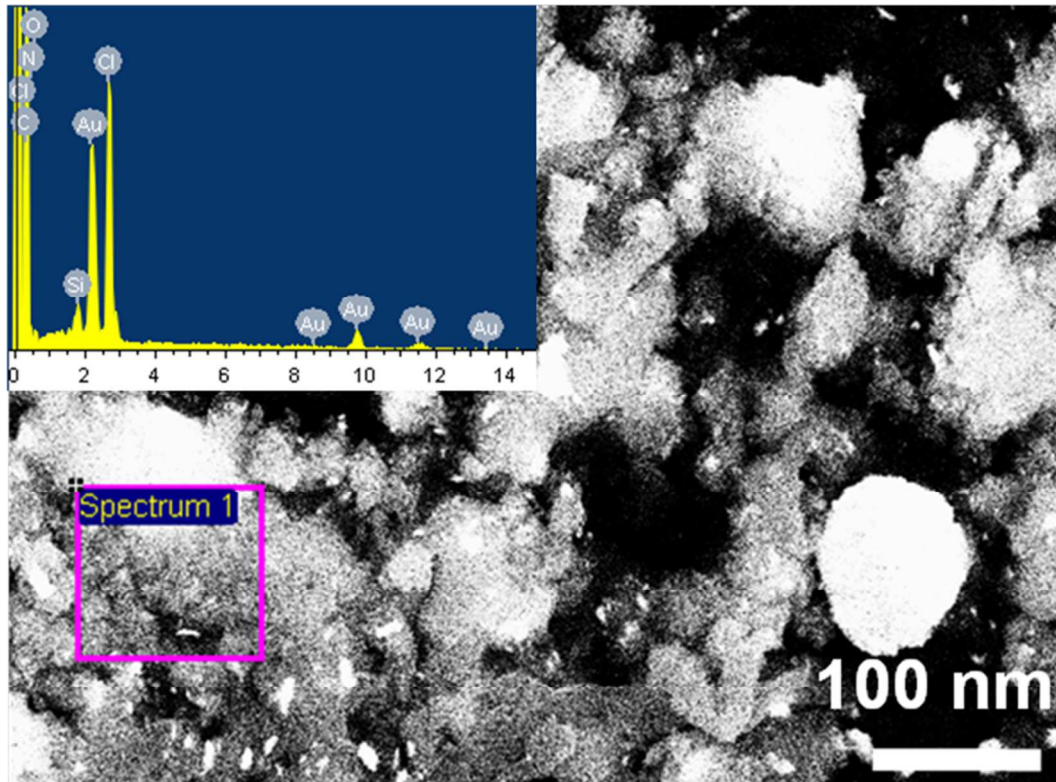


Figure 3

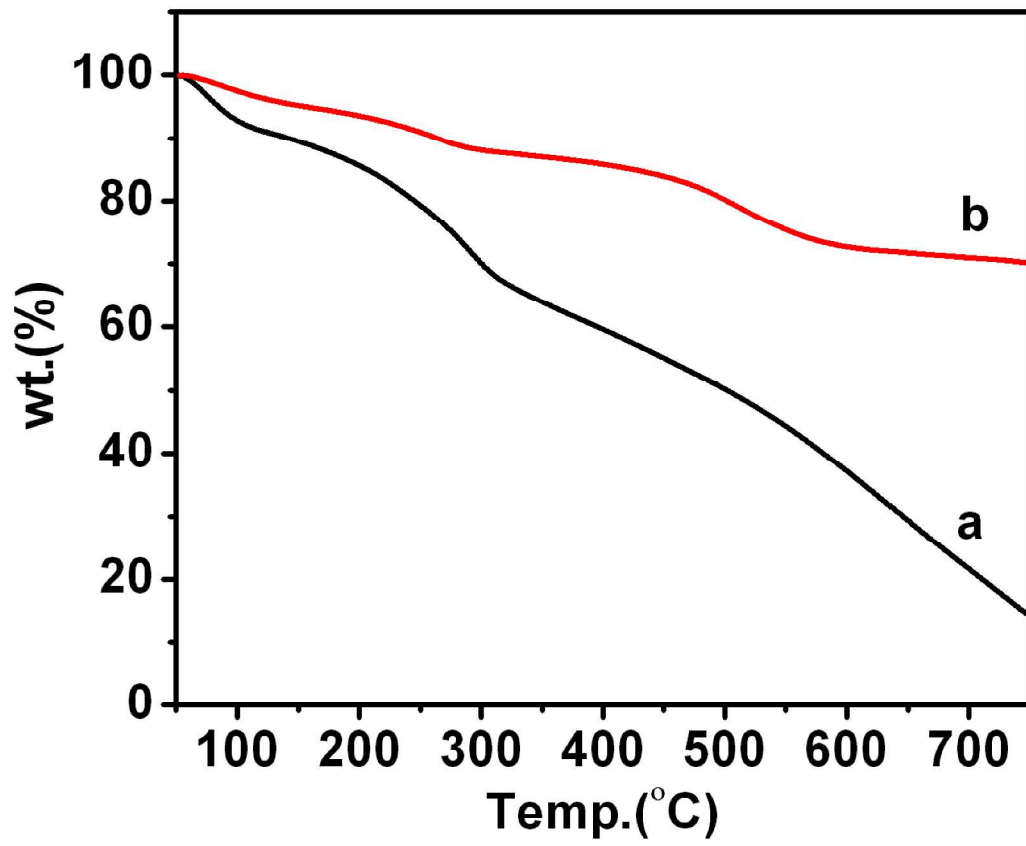


Figure 4

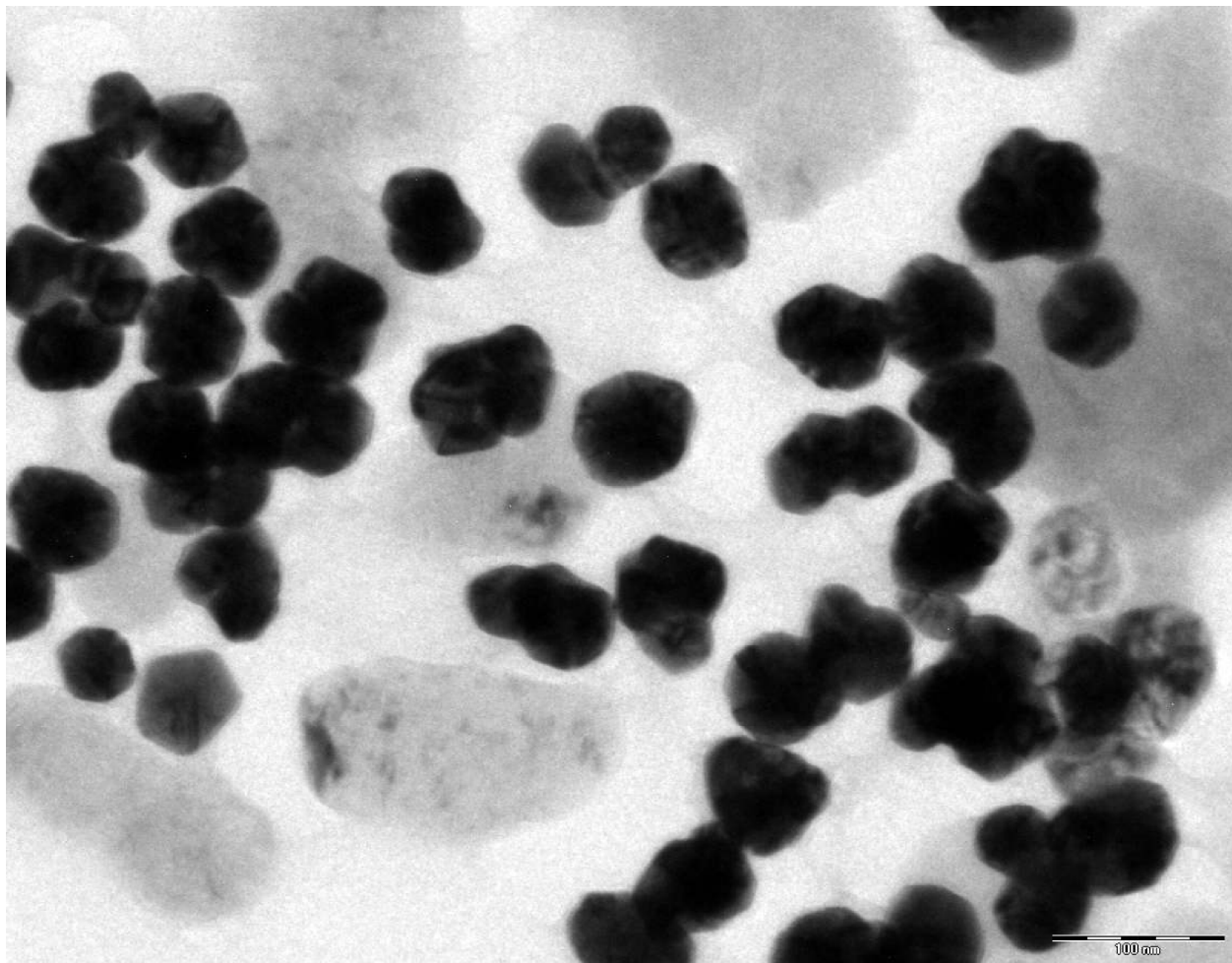


Figure 5

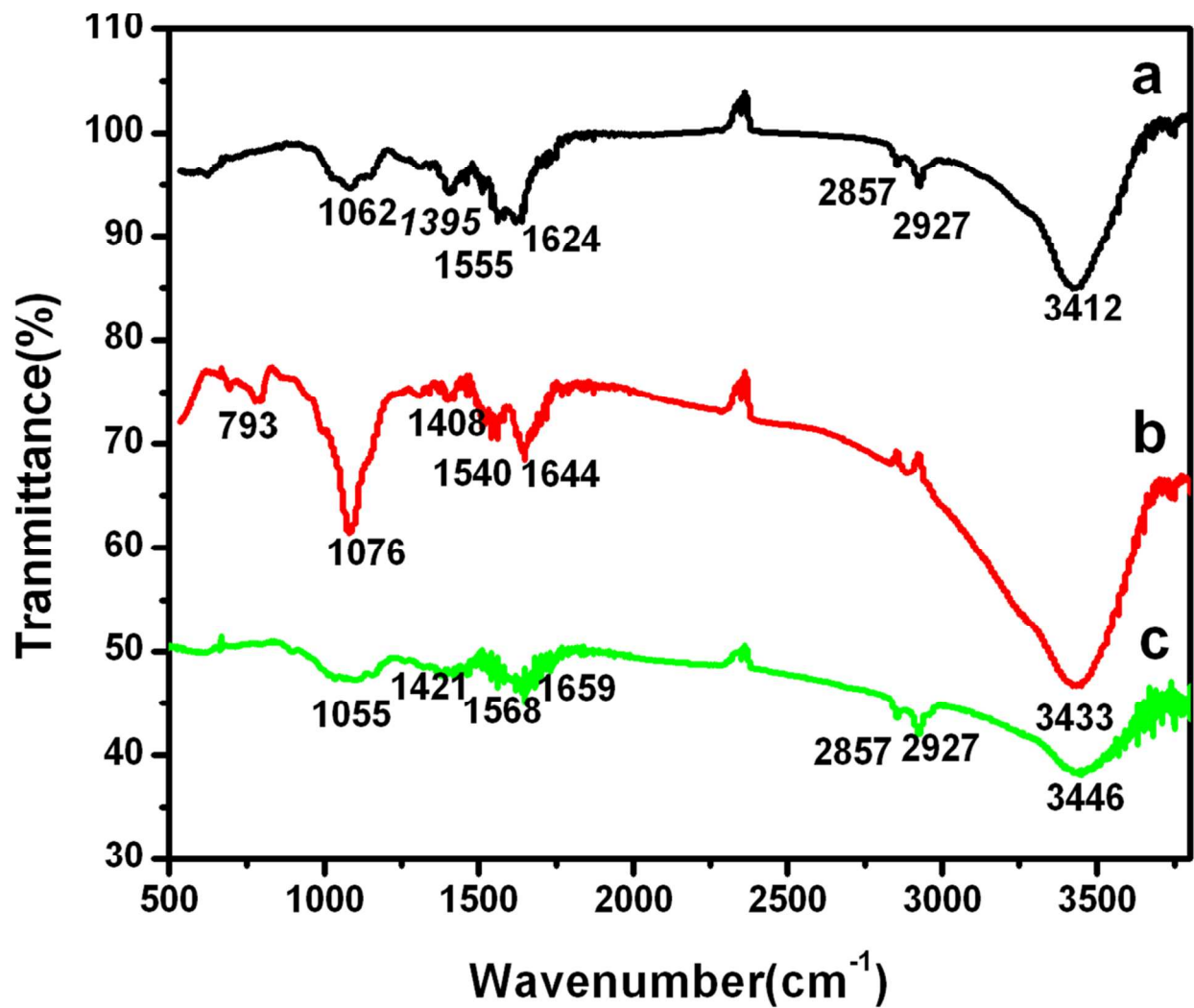


Figure 6

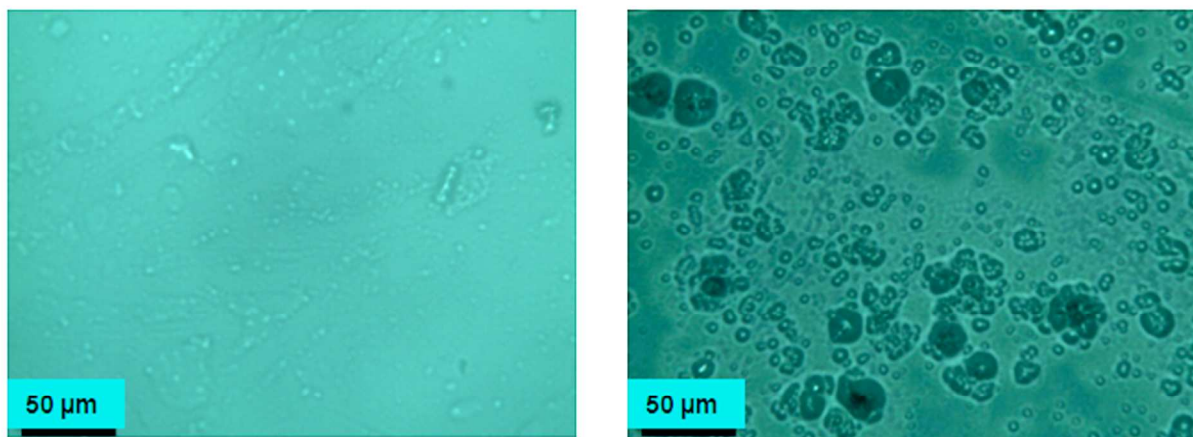


Figure 7

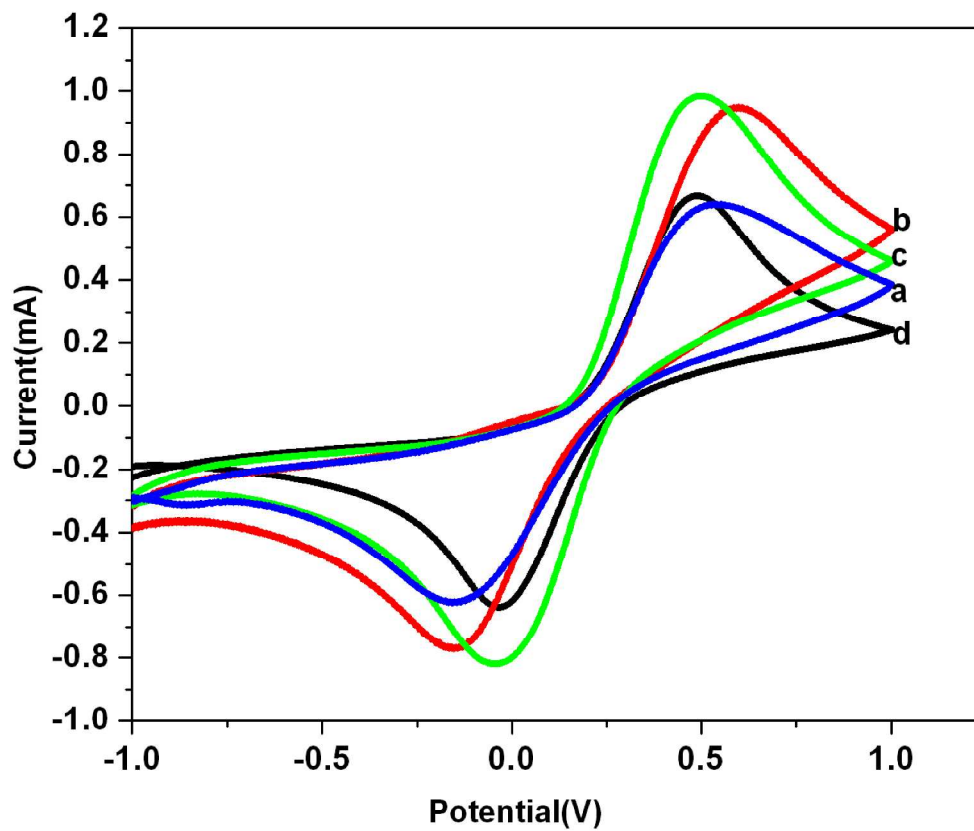


Figure 8

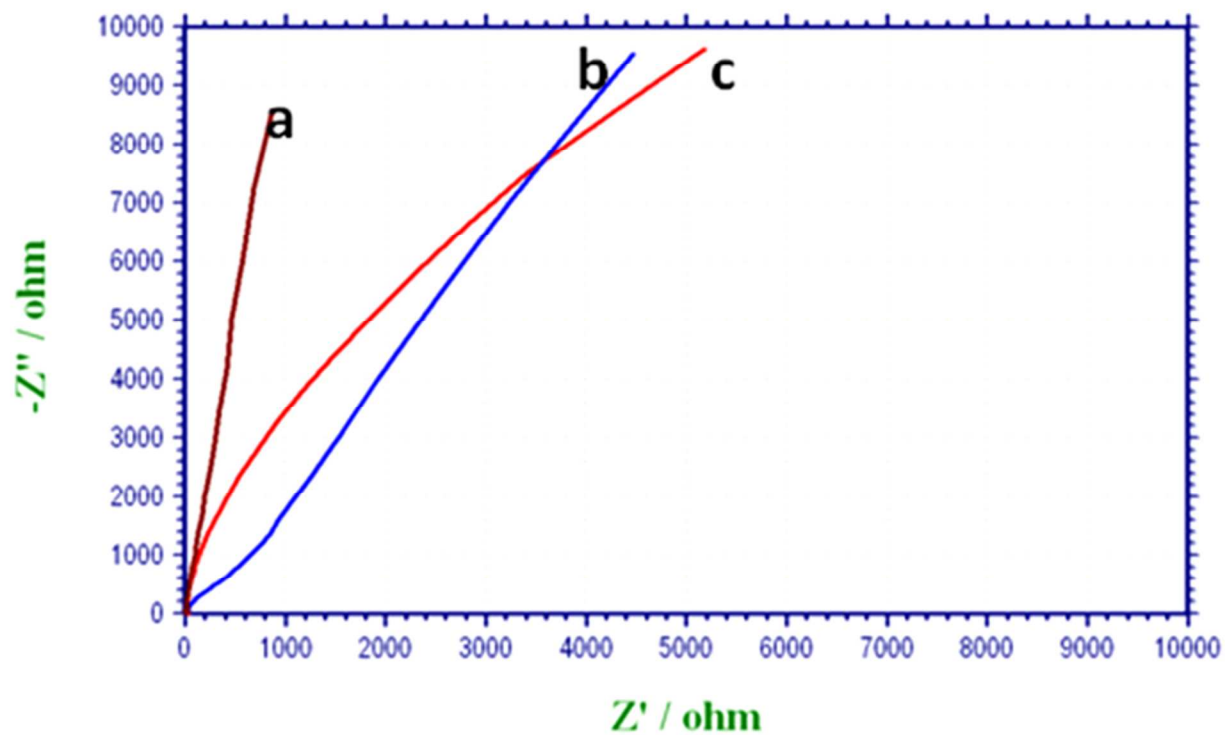


Figure 9

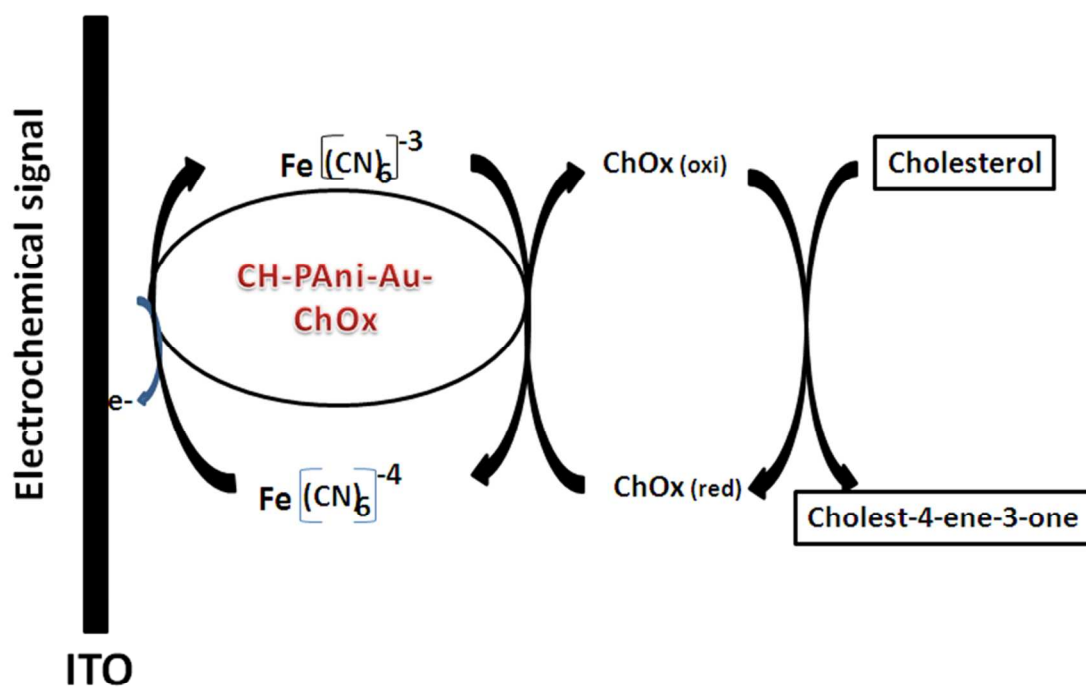


Figure 10

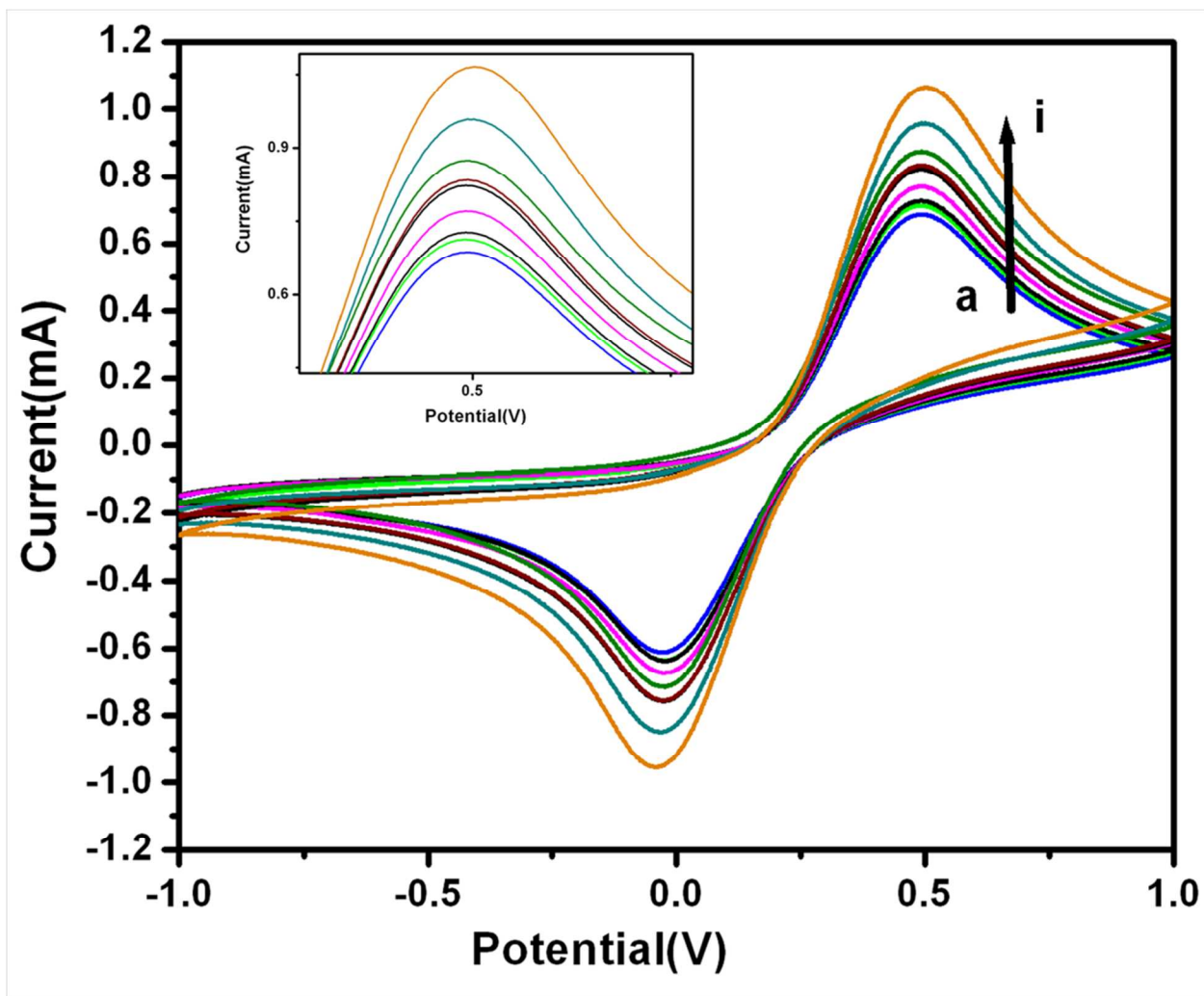


Figure 11

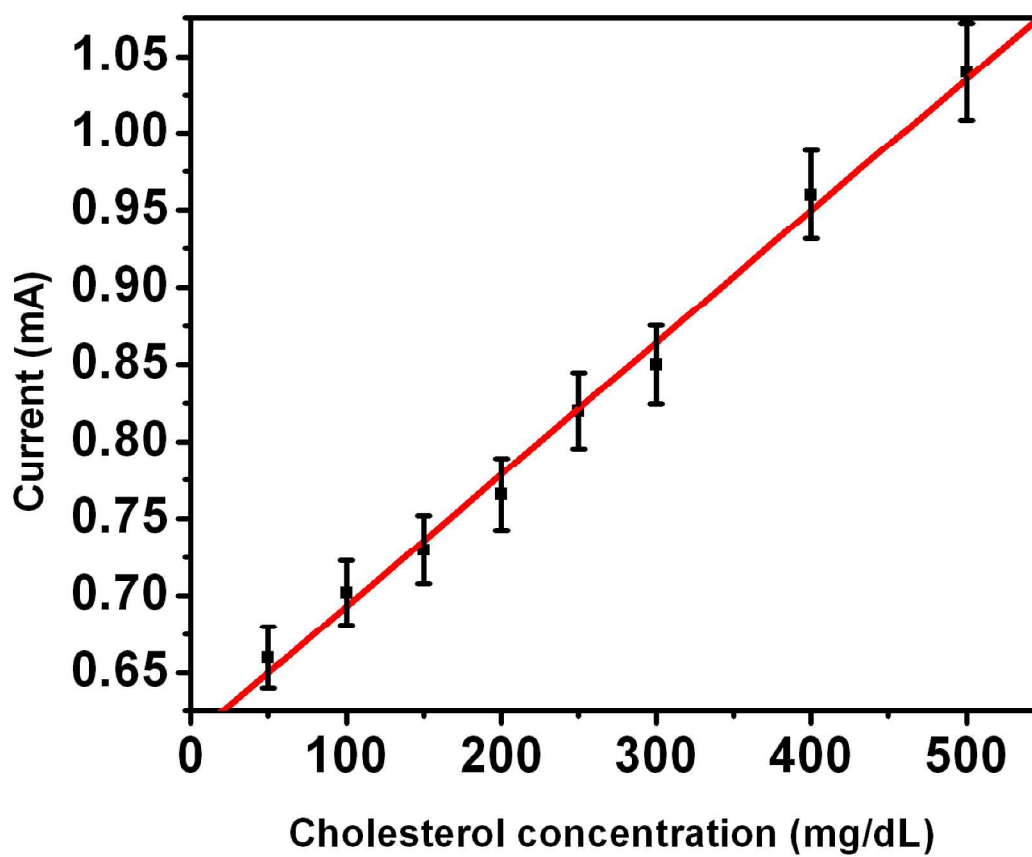


Figure 12

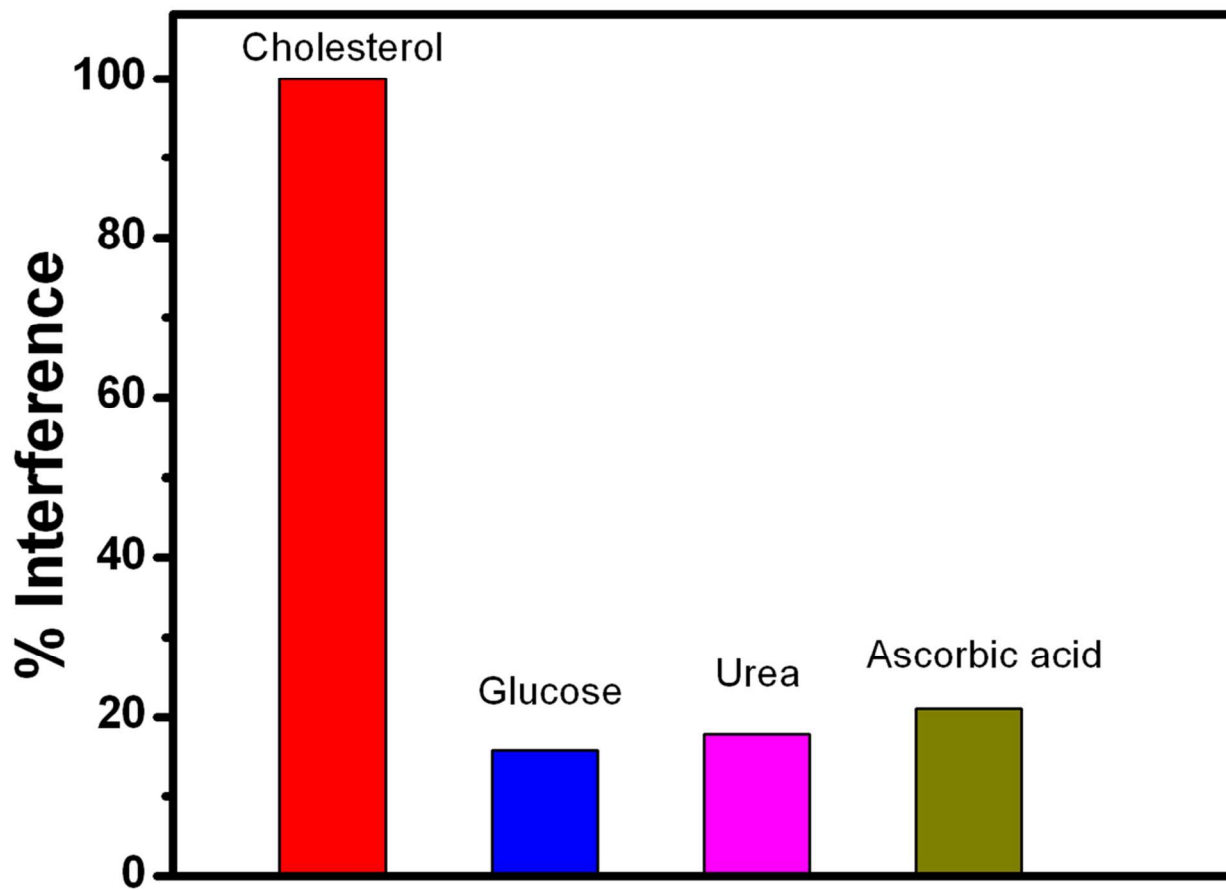


Figure 13

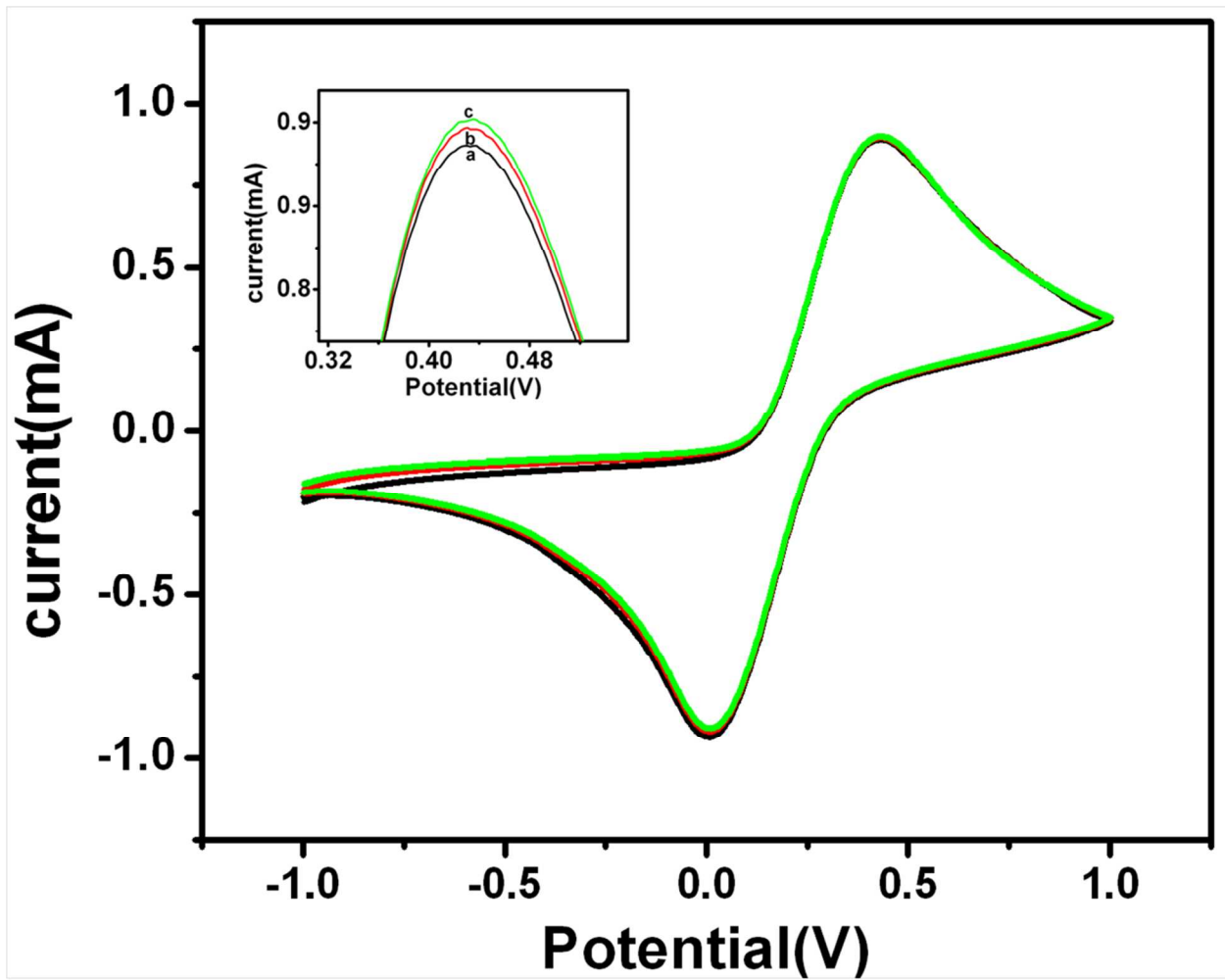


Figure 14

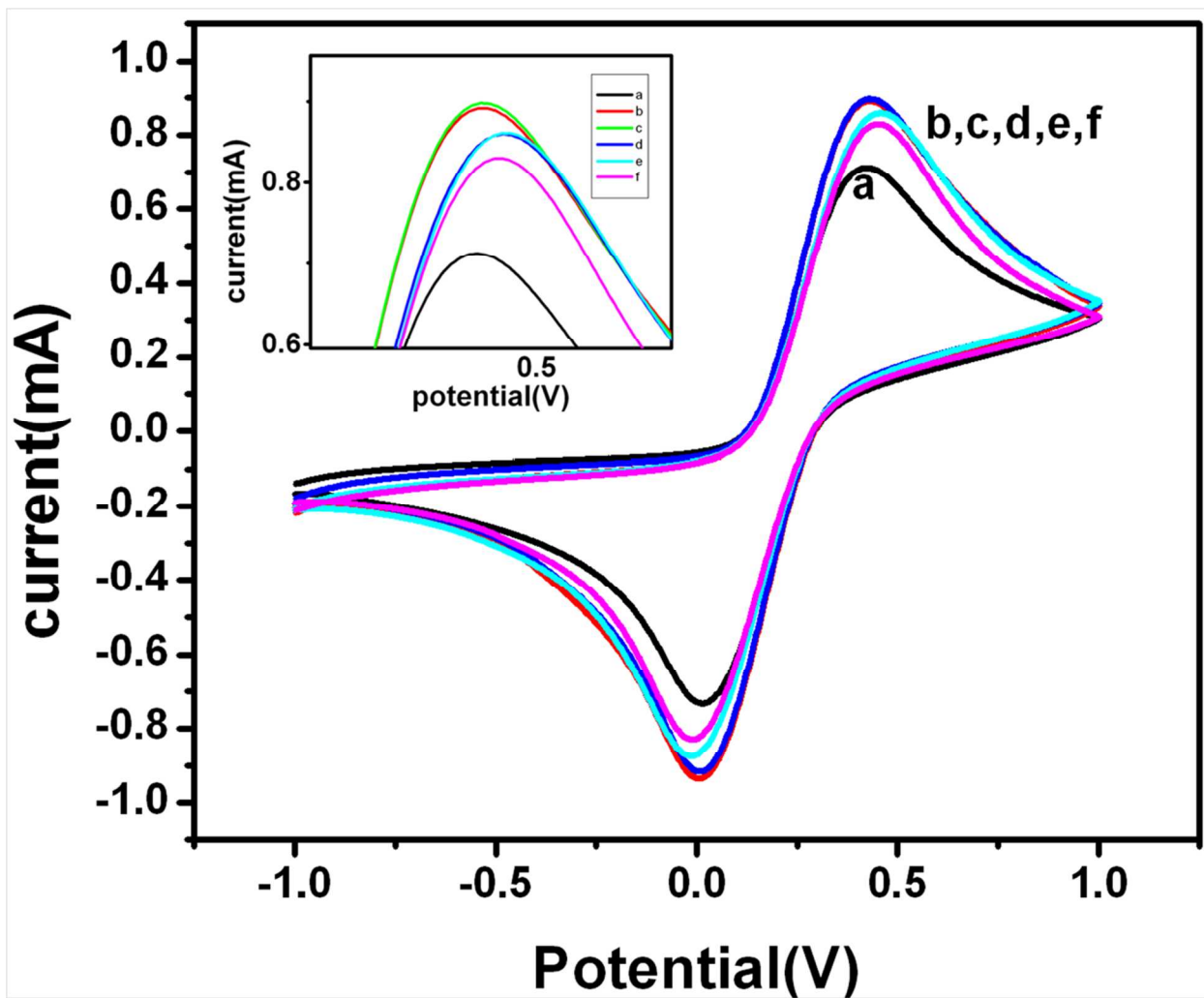


Figure 15